Stochastic Models and Simulations of Phototaxis

Amanda Galante
University of Maryland, College Park
agalante@cscamm.umd.edu
Susanne Wisen
Carnegie Institution for Science, Stanford
swisen@stanford.edu
Devaki Bhaya
Carnegie Institution for Science, Stanford
dbhaya@stanford.edu
Doron Levy
University of Maryland, College Park
dlevy@math.umd.edu

Certain microorganisms undergo phototaxis, that is they migrate toward light. This motion is typically associated with fingering patterns similar to those that develop in unstable fronts. In this work, we are concerned with the phototactic organism *Synechocystis sp.*, a cyanobacterium that has been studied in a laboratory setting in order to understand the functionality of the cell and how the motion of individual cells is translated into emerging patterns on macroscopic scales. Experimentally, it is observed that a critical number of cells are necessary for the detection of the direction of light and for initiating a directional movement. While significant advances have been made in studying the ways by which the bacteria can detect the light and move towards it, it is not well understood how do these unicellular organisms identify the direction of the light. It is also not understood how the motion of the individual cells and the cell-to-cell interactions are then translated into the observed complex patterns. Using the experimental data on *Synechocystis sp.*, we were able to identify a collection of rules for the local movement of cells on small length- and time-scales. These observations were then used to develop stochastic mathematical models, which integrate local rules of motion (on small scales), with the global, large-scale forcing of

the light source. Simulations of the mathematical models provide interesting insights on the relative role of the local and global forcing. They also provide a tool for studying the critical threshold that determines whether local aggregation patterns form or not. Our mathematical modeling results are shown to be in agreement with the available experimental data.

1 Introduction

Phototaxis is the movement of certain microorganisms toward a light source. For unicellular bacteria, phototaxis expresses itself with populations of cells migrating in the direction of light, typically forming finger-like patterns. The movement and pattern formations have been experimentally shown to depend on the density of cells, wavelength of light, and the properties of the surface [2]. They are thought to depend on cellular signals and intercellular interactions. *Synechocystis sp.* is known to contain photoreceptors that are capable of sensing light. They also contain pili, hairlike appendages, of different diameters. Some pili are used as the motion apparatus, while the role of other pili is less known, though it is likely that they play some role in signaling between bacteria. Phototaxis in *Synechocystis sp.* is a complex and well-regulated process. Several mutants in phototaxis have been identified [1] and yet a complete understanding of the signals and intercellular interactions that control the emergent behaviors of phototactic cells is still lacking.

The mathematical modeling community has done relatively little work in modeling phototaxis. There is a large body of work on chemotaxis, the phenomenon of cells moving toward a chemokine (e.g. see [12] and the references therein). The assumptions and analysis of the Couzin-Viscek algorithm, a flocking model in which fish move in the average direction of their neighbors within a given radius, are also applicable [5, 13, 6]. However, the emergent behaviors and cellular structure of phototactic cells are quite different from chemotactic cells and flocking animals and fish. So far, only a handful of models of phototaxis have been developed, e.g. [3, 4, 7, 8, 9, 10]. While these models incorporate group dynamics, they do not capture the intricate quasi-random pattern of motion, which is the focus of this work.

In this work, after studying the motion of individual bacteria, we develop a model based on rules of observed local interaction. Cells appear to incorporate into their motion, the location of neighboring cells. Accordingly, we formulate a stochastic model that allows cells to move in directions that are different than a simple random motion or a uniform migration towards the light source. Our local-interactions model is presented in §3.2. Global forcing due to a light source is incorporated into the model in §3.3. A variety of simulations of our stochastic models are demonstrated in §4. Concluding remarks are provided in §5.

2 Experimental observations of phototaxis

Experimental results were obtained by viewing image sequences of plated cyanobacteria *Synechocystis sp.* under different light and concentration conditions. The experimental data leads to the following observations:

1. **Pattern formation.** Groups of cells form fingers reaching in the direction of the light source.
2. **Surface memory.** Cell movement is predominantly constrained to the surface which has been pre-wetted by other cells.
3. **Delayed motion.** Cells do not begin moving until they have been exposed to light for at least a few hours. Motion towards light is typically observed in areas where cells aggregate.
4. **Quasi-random motion.** Not all cells ultimately move toward light. Some cells move in a persistent pattern, in a direction that changes frequently, with no apparent bias towards light. Many cells become stuck at the interface of the wetted and non-wetted surface.

Some of these observations are shown in Figure 1. All figures are snapshots of the experimental results. The bacteria are the white dots. In Fig. 1(a) and Fig. 1(c), small aggregations of cells can be seen as well as cells stuck at the wetted/non-wetted surface interface. In Fig. 1(b) isolated cells (perhaps due to the lack of surface wetting) are observed. Fig. 1(a), also demonstrates the initiation of a wide finger pattern formation.

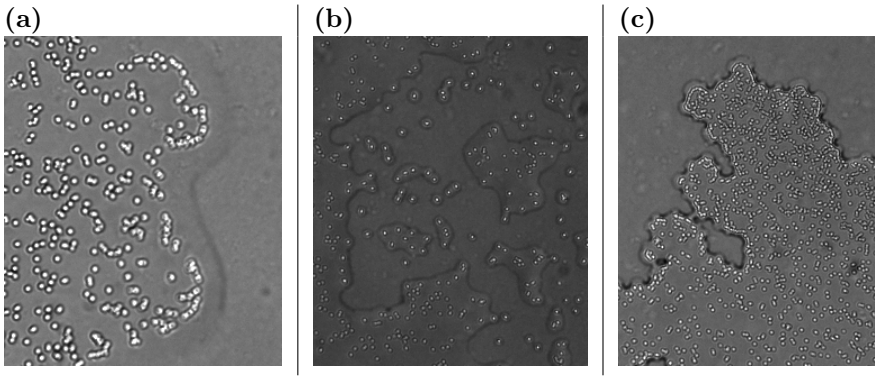

Figure 1: Experimental results illustrating (a) fingering, (b) surface dependence, and (c) aggregation

3 A mathematical model for phototaxis

Based on the experimental observations discussed in §2, we focus our attention on the quasi-random mode of motion (observation (4)). The experimental obser-

vations lead to a set of rules that can be used to describe the local interactions between cells. Global forcing on the motion, due to the external light source, can then be added to the system.

3.1 Model assumptions

In order to develop a mathematical model of the quasi-random state of cell motion, we make several assumptions. First, we assume that cells can identify the location of their neighbors. In making this assumption, we assume that there is an underlying communication mechanism between cells —possibly by signaling, local force sensing, or physical interaction. For the purpose of this model, the actual mechanism of communications is of no interest. The size of the neighborhood, in which cells can communicate with each other, will be taken as one of the model parameters. Additionally, we assume that cells are not necessarily all alike, i.e., it is possible for cells to have different traits.

3.2 Local interactions

We start by modeling the local interactions between cells in low density areas. Our model is written as a discrete time interacting particle system. At any given point in time, we assume that every cell may move according to one of the following three options (shown in Figure 2):

(a) a cell may continue to move without changing its previous direction

(b) a cell can stop moving

(c) a cell may orient itself. In this case it will moves in the direction of one of its neighboring cells. The candidate neighboring cells must be within a certain interaction distance (shown as the dotted circle in Figure 2(c)).

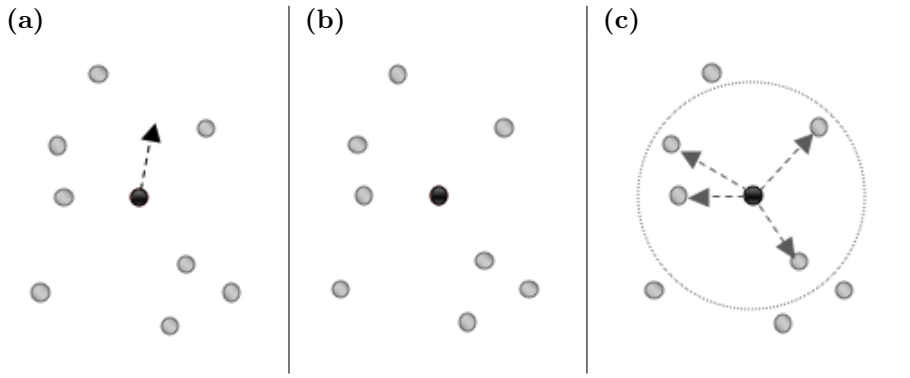

Figure 2: Local interaction model with (a) persistence of motion in previous direction, (b) stationary, and (c) motion in the direction of a neighbor

To formulate the model, we consider N cells in $\mathbb{R}^2$. Each cell i has a direction $\theta_i(t)$ and a velocity $v_i(t)$. The time is assumed to be discrete with $t \in \mathbb{N}$. The position of cell i at time t is denoted by $x_i(t)$. Similar variables are considered in a recent discrete model of chemotaxis [11].

The initial velocities of the particles are either 1 or 0. The angle θ_i is updated by allowing a cell i to maintain its current direction with probability a or to switch its direction toward one of its neighboring cells with probability $1-a$. The neighborhood in which a cell can sense a neighboring cell is defined as a ball of radius D. Thus, the angle of motion is updated as

$$\theta_i(t+1) = \begin{cases} \theta_i(t), & \text{with probability } a, \\ \eta_j, & \text{with probability } \frac{1-a}{n_i} \text{ for } j \text{ s.t. } x_j \in B_D(x_i), \end{cases} \tag{1}$$

where $B_D(x_i)$ is a ball of radius D centered at x_i, n_i is the number of cells with position x_j contained in $B_D(x_i)$, i.e. $||x_i(t) - x_k(t)||_2 < D$, and η_j is the angle of the vector pointing from particle i to particle j. The velocities are updated according to the following rule: v_i does not change with probability b. With probability $1-b$ the velocity v_i switches between 0 and 1. This is formulated as

$$v_i(t+1) = \begin{cases} v_i(t), & \text{with probability } b, \\ 1 - v_i(t), & \text{with probability } 1-b. \end{cases} \tag{2}$$

In this way, the velocity is either 1 (in which case the cell continues to move) or 0 (in which case it stays in place). After calculating the angle and the velocity for every cell, the positions $\{x_i\}$ of the cells are updated according to

$$x_i(t+1) = x_i(t) + v_i(t) \begin{bmatrix} \cos(\theta_i(t+1)) \\ \sin(\theta_i(t+1)) \end{bmatrix}. \tag{3}$$

3.3 Global forcing

Global forcing can be incorporated into our stochastic model of local interactions in different ways. It is experimentally observed that not all cells move in the direction of the light. This means that it is possible that not all cells are capable of identifying the direction of the light. Accordingly, we propose two models that incorporate the individual response of cells to the light. In the first model (Model A) we assume that all cells are capable of identifying the direction of the light. In the second model (Model B) we assume that only a subset of the colony is capable of identifying the direction of light. In both models, cells that are capable of sensing the direction of light are not assumed to automatically move in that direction. Rather, when moving, in addition to the local-interactions rules, they have the additional option of moving towards light. See Figure 3.

Model A In this model, every cell is capable of sensing the direction of light. We modify equation (1) to allow the cells to move in the direction of light θ_0 with probability c.

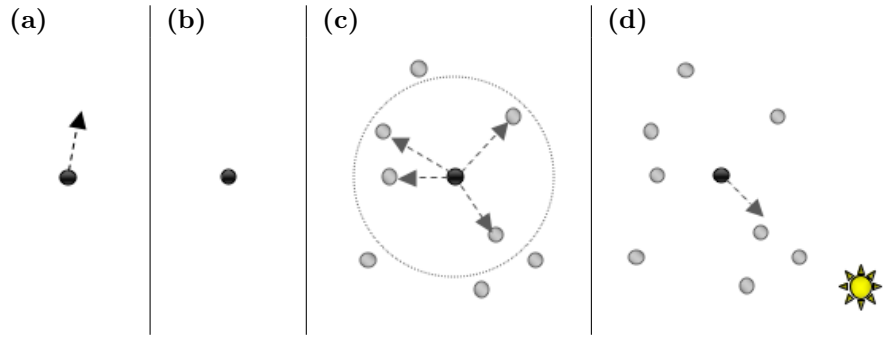

Figure 3: (a) - (c) Local interaction model and (d) Global forcing in direction of light

$$\theta_i(t+1) = \begin{cases} \theta_i(t), & \text{with probability } a, \\ \theta_0, & \text{with probability } c, \\ \eta_j, & \text{with probability } \frac{1-a-c}{n_i} \text{ for } j \text{ s.t. } x_j \in B_D(x_i), \end{cases} \tag{4}$$

Note that in this case, we assume that the light source is far away so that the direction of light is identical for all cells on the plate.

Model B In this model, only a subset of cells are capable of sensing the direction of the light source. To model this, cells are randomly assigned to be of type *leader* or type *normal*. Cells of the *leader* subtype update directions according to equation (4). Cells of the *normal* subtype update directions according to equation (1). The ratio of *leader* to *normal* cells is a model parameter. Its effect is studied in the numerical simulations.

4 Results and discussion

In this section we present results of simulations of our models. In all cases, we assume that the cells are constrained to a 200 pixel diameter disc in $\mathbb{R}^2$. Cells are allowed to move in any direction that is allowed by the model within the disc but are not allowed to cross its boundary to the exterior of the domain. Such a constraint is consistent with the observed behavior of cells on the wetted area of a plate on small time-scales. On larger time scales, in the absence of a directed light source, cells diffuse radially. In each simulation, we set the number of particles N to be either 250 or 500. The particles are represented in each simulation by circles of radius 2 pixels. For each set of parameters, we consider two different interaction distances: $D = 5$ and $D = 10$ pixels. The interaction distance is shown with a red bar of the appropriate pixel length in the upper left corner of each figure. In all simulations we assume that the probability of directional persistence, a, is 0.8. The probability of switching velocity from 1

to 0 or 0 to 1, b is set as 0.5. For both global interaction models **A** and **B**, the probability of a cell moving in the direction of light at any time step, c, is 0.005. For the global interaction model **B**, unless otherwise stated, the probability of a cell being able to sense the direction of light is 0.5, i.e., is, the ratio of *leader* to *normal* cells is 1:1. The group of *leader* cells are identified as unfilled circles in the simulations.

In the local interaction model, cells are capable of moving toward a random neighbor, persisting in their chosen direction, or being stationary. Simulations of the local interactions base model for $N = 250$ and 500 and for $D = 5$ and 10 are shownin Figure 4. The snapshots for each simulation are taken at times $t = 0, 50$ and 350. The initial positions, directions and velocities of the cells are identical for Fig. 4(a) and Fig. 4(e) with $N = 250$ and for Fig. 4(g) and Fig. 4(j) with $N = 500$. The same initial conditions are used in all of the following simulations. Note that in the case $D = 5$, cells become temporarily fixed on the edge of the circle, visible in Fig. 4(b), Fig. 4(c), Fig. 4(h) and Fig. 4(i). These cells occasionally move back into the domain, but generally, spend most of the time on the boundary. We also observe large aggregations forming for $D = 10$ in Fig. 4(f) and Fig. 4(l) and small aggregations forming for $D = 5$ in Fig. 4(c) and Fig. 4(i). All images illustrate the observed quasi-random motion of cells that is observed experimentally.

In the global model **A**, all cells are aware of the direction of light but only have a 0.5% chance of choosing to orient in the direction of the light at each time step. Note that if a particle is moving in the direction of light (or in any other direction), with each progressive time step, the cell will persist in that direction with probability 0.8. Simulations of this joint global-local interaction model are shown in Figure 5. The initial conditions $\{x_i(0), \theta_i(0), v_i(0)\}$ are the same for each set of values of N and D as in Figure 2 (see Figs. 5(a), 5(d), 5(g) and 5(j)). The direction of light in these simulations is at the lower right corner ($\theta = -\pi/4$). For $D = 5$, we still see cells that become fixed on the edge of the circle, even for $t = 1000$ (see Figs. 5(b), 5(c), 5(h) and5(i)). For $D = 10$, we still observe the formation of large aggregations. In comparing Fig. 5(c) with Fig. 5(f) and Fig. 5(i) with Fig. 5(l) at $t = 1000$, the mass movement in the direction of light is clearly observable for $D = 5$ but not in the case of a larger neighborhood, i.e., $D = 10$. The migration toward light appears to be greater for the smaller number of particles $N = 250$ compared with $N = 500$ as can be seen in Figs. 5(c) and 5(i).

The global model **B** combines the local interaction model with only a fraction of cells that are allowed to intentionally pursue the direction of the light source as in global model **A**. Simulations of this global model with *leader* to *normal* cell ratio of 1:1 are shown in Figure 6. The initial conditions of variables $\{x_i(0), \theta_i(0), v_i(0)\}$ are identical to those in Figs. 6(a), 6(c), 6(g), and 6(j). The cells which are aware of the direction of light are identified in the simulation as open red circles. In these simulations, as the number of time steps increases, one expects to see general migration of cells toward the lower right hand quadrant of each circle as happened with **A**. Similar to Figure 5, this trend is not apparent

at $t = 500$, in Figs. 6(b), 6(e), 6(h) and 6(k), or at $t = 1000$ and $D = 10$, in Figures 6(f) and 6(l). It can be observed in the distribution of red *leader* cells for $D = 5$ at $t = 1000$ in Fig. 6(c) and Fig. 6(i). The distribution of *normal* cells appears to be uniform in each of these snapshots.

Large time simulations of each models are shown in Figure 7. Note that for the local interaction model alone, in Figs. 7(a), 7(d), 7(g) and 7(j), even though cells are still moving, the pattern of cells does not change significantly between $t = 3000$ and $t = 9999$. In the global model **A** (shown in Figs. 7(b) and 7(e) with $D = 5$), while most of the cells aggregate along the side of arc of the circle that is closest to the light source, cells are still capable of escaping back into the domain. Whereas, in Fig. 7(h) and Fig. 7(k) with $D = 10$, most of the cells aggregate along the leading edge as the number of time steps increases. In the global model **B** with $D = 5$ (shown in Figs. 7(c) and 7(f)), the *leader*-type cells move towards the leading edge but do not appear to gather along the edge in large numbers. Instead, they end up spreading throughout the domain. The *normal*-type cells are spread somewhat uniformly. These patterns are indicative of the observed quasi-random motion of cells. For $D = 10$ at $t = 3000$, the aggregations of *leader*- and *normal*-type cells are somewhat uniform in Fig. 7(i), but most aggregates tend towards the light source as t increases as can be seen in Fig. 7(l).

Finally, we study the impact of the ratio of *leader* to *normal* cells in the global model **B**. Simulations are shown in Figure 8. We consider 3 cases in which the ratios are 3:1, 1:1, and 1:3. In addition, we consider the case where all cells are *leader* cells, as in global model **A**. The initial conditions $\{x_i(0), \theta_i(0), v_i(0)\}$ are taken to be the same as before. They are shown in Figs.8(a), 8(d), 8(g), and 8(j). In all simulations $D = 5$ and $N = 250$. The results of the simulations are consistent with the characterization of the quasi-random motion. We also observe that cells get stuck along the entire edge of the circle. A migration of *leader* cells toward light, in all three ratios, (shown in Figs. 8(b), 8(e), and 8(h)) is somewhat visible and is very apparent in Figs. 8(c), 8(f), and 8(i). In each of these cases, the distribution of *normal* cells appears to be uniform. Comparisons of these simulations with experimental data to the simulation where all cells are *leader*-type cells supports the hypothesis that cells may not be all alike. It seems feasible that only a portion of the cells are capable of identifying the direction of the light source.

5 Conclusions and future directions

In this work we presented the first discrete-time, stochastically interacting particle model, for describing local interactions between phototactic cells in which cells can stochastically choose a neighboring cell to follow. Our results qualitatively match the experimental results in the region of quasi-random bacterial motion. We varied a couple factors in each simulation: the interaction distance, D, and the number of particles in simulation, N.

The simulations of the local interaction model illustrated that particle may

aggregate. Some particles ended up sticking to the boundary of the domain. Both traits have been observed experimentally. The simulation results also suggest that the interaction distance of particles D is likely to be small (as the simulations for $D = 5$ seem to be a better qualitative match to the experiments when compared with $D = 10$.) We hypothesize that this parameter is related to a physical characteristic of cells. The number of particles affects the size of aggregations but the general patterns of motion are the same. Further studies should be done to determine the minimum and maximum densities for which this model qualitatively replicates experimental data. The size of the particles will likely become a relevant factor for simulations as the number of particles increases.

We incorporated global forcing due to a light source into our model by stochastically allowing cells to move in the direction of light (in addition to the other local rules of motion). We considered two scenarios: one in which all cells are capable of identifying the direction of light and a second case in which only a fraction of the cells are capable of identifying the direction of light. When all cells are capable of identifying the direction of light, they all tend to migrate in that direction. However, on large time scales, for a smaller interaction distance it is still possible to see some quasi-random motion. This is consistent with the experimental data.

When comparing all models on large time scales, a quasi-random motion seems to be more present in the models where not all cells are capable of detecting the direction of light. This issue should be further investigated experimentally, but the evidence presented in this paper strongly indicates the possibility that there is a substantial subpopulation of cells that is not capable of detecting the direction of the light source.

Acknowledgements

This work was supported in part by the joint NSF/NIGMS program under Grant Number DMS-0758374 The work of AG and DL was supported in part by Grant Number R01CA130817 from the National Cancer Institute. The content is solely the responsibility of the authors and does not necessarily represent the official views of the National Cancer Institute or the National Institutes of Health.

Bibliography

[1] Bhaya, Devaki, Akiko Takahashi, Payam Shahi, and Arthur R Grossman, "Novel Motility Mutants of *Synechocystis* Strain PCC 6803 Generated by In Vitro Transposon Mutagenesis", *Journal of Bacteriology* **183** (2001), 6140–6143.

[2] Bhaya, Devaki. "Light matters: phototaxis and signal transduction in unicellular cyanobacteria", *Molecular Microbiology* **53** (2004), 745–754.

[3] Bhaya, Devaki, Doron Levy, and Tiago Requeijo, "Group dynamics of phototaxis: Interacting stochastic many-particle systems and their continuum limit", *Hyperbolic Problems: Theory, Numerics, Applications* (2008), 145–159.

[4] Burriesci, Matthew, and Devaki Bhaya, "Tracking phototactic responses and modeling motility of *Synechnocystis sp.* strain PCC6803", *Journal of Photochemistry and Photobiology B: Biology* **91** (2008), 77–86.

[5] Couzin, Iain D, Jens Krause, Richard James, Graeme D Ruxton, and Nigel R Franks, "Collective memory and spatial sorting in animal groups", *Journal of Theoretical Biology* **218** (2002), 1–11.

[6] Degond, Pierre, and Sébastien Motsch, "Continuum limit of self-driven particles with orientation interaction", *Mathematical Models and Methods in Applied Sciences* **18** (2008), 1193–1215.

[7] Ha, Seung-Yeal, Kiseop Lee, and Doron Levy, "Emergence of time-asymptotic flocking in a stochastic cucker-smale system", *Communications in Mathematical Sciences* **7** (2009), 453–469.

[8] Levy, Doron, and Tiago Requeijo, "Modeling group dynamics of phototaxis: from particle systems to PDEs", *Discrete and Continuous Dynamical Systems - Series B* **9** (2008), 103–128.

[9] Levy, Doron, and Tiago Requeijo, "Stochastic models for phototaxis", *Bulletin of Mathematical Biology* **70** (2008), 1684–706.

[10] Levy, Doron, and Seung-Yeal Ha, "Particle, kinetic and fluid models for phototaxis", *Discrete and Continuous Dynamical Systems - Series B* **12** (2009), 77–108.

[11] Nicolau, Dan V, Judith P Armitage, and Philip K Maini, "Directional persistence and the optimality of run-and-tumble chemotaxis", *Computational Biology and Chemistry* **33** (2009), 269–74.

[12] Tindall, Marcus J, Philip K Maini, Steven L Porter, and Judith P Armitage, "Overview of mathematical approaches used to model bacterial chemotaxis II: bacterial populations", *Bulletin of Mathematical Biology* **70** (2008), 1570–1607.

[13] Vicsek, Tamás, András Czirók, Eshel Ben-Jacob, Inon Cohen, and Ofer Shochet, "Novel type of phase transition in a system of self-driven particles", *Physical Review Letters* **6** (1995), 1226–1229.

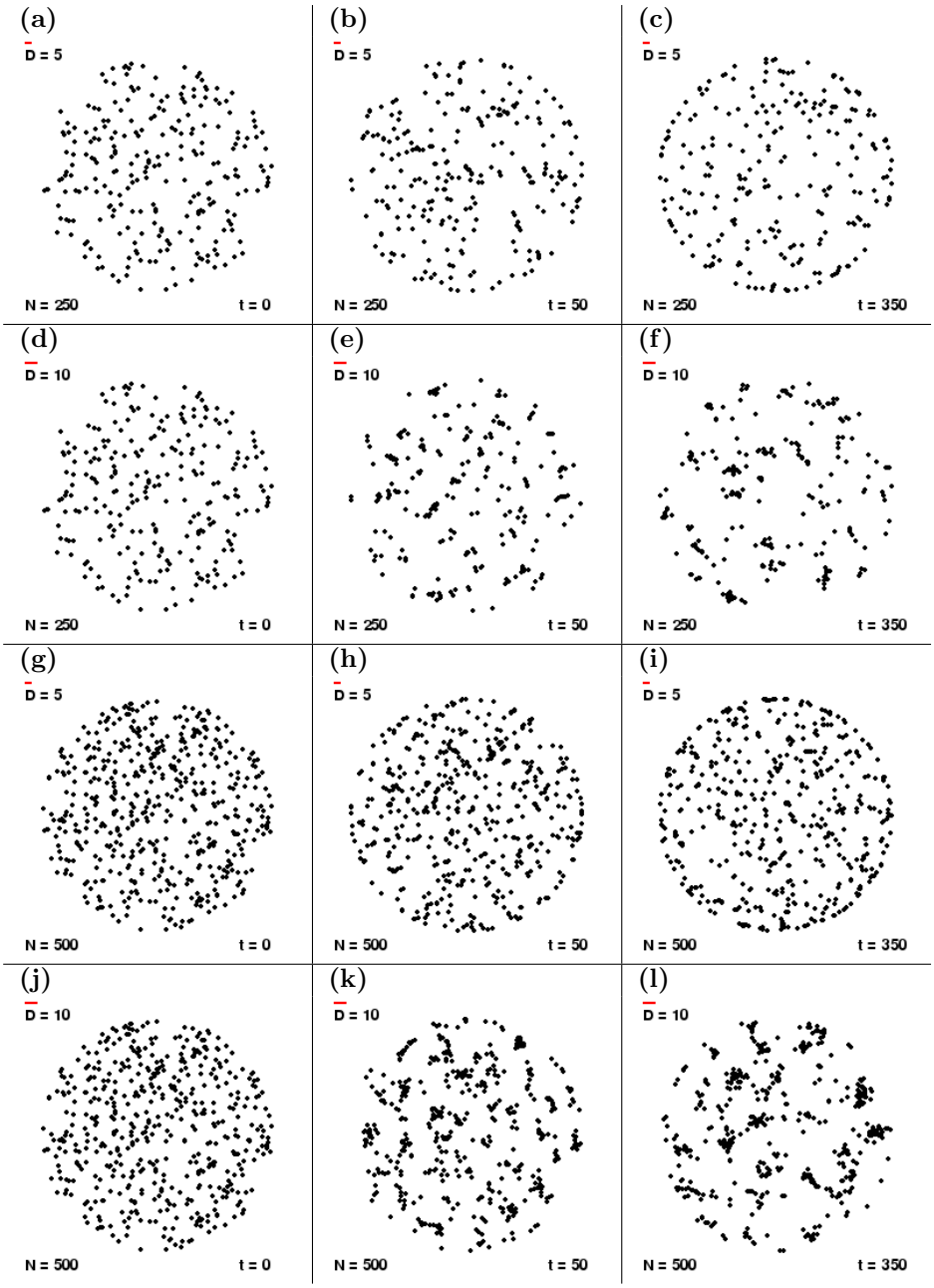

Figure 4: Local interaction model at $t = 0, 50, 350$ time steps with (a)-(c) $D = 5$, $N = 250$, (d)-(f) $D = 10$, $N = 250$, (g)-(i) $D = 5$, $N = 500$, and (j)-(l) $D = 10$, $N = 500$.

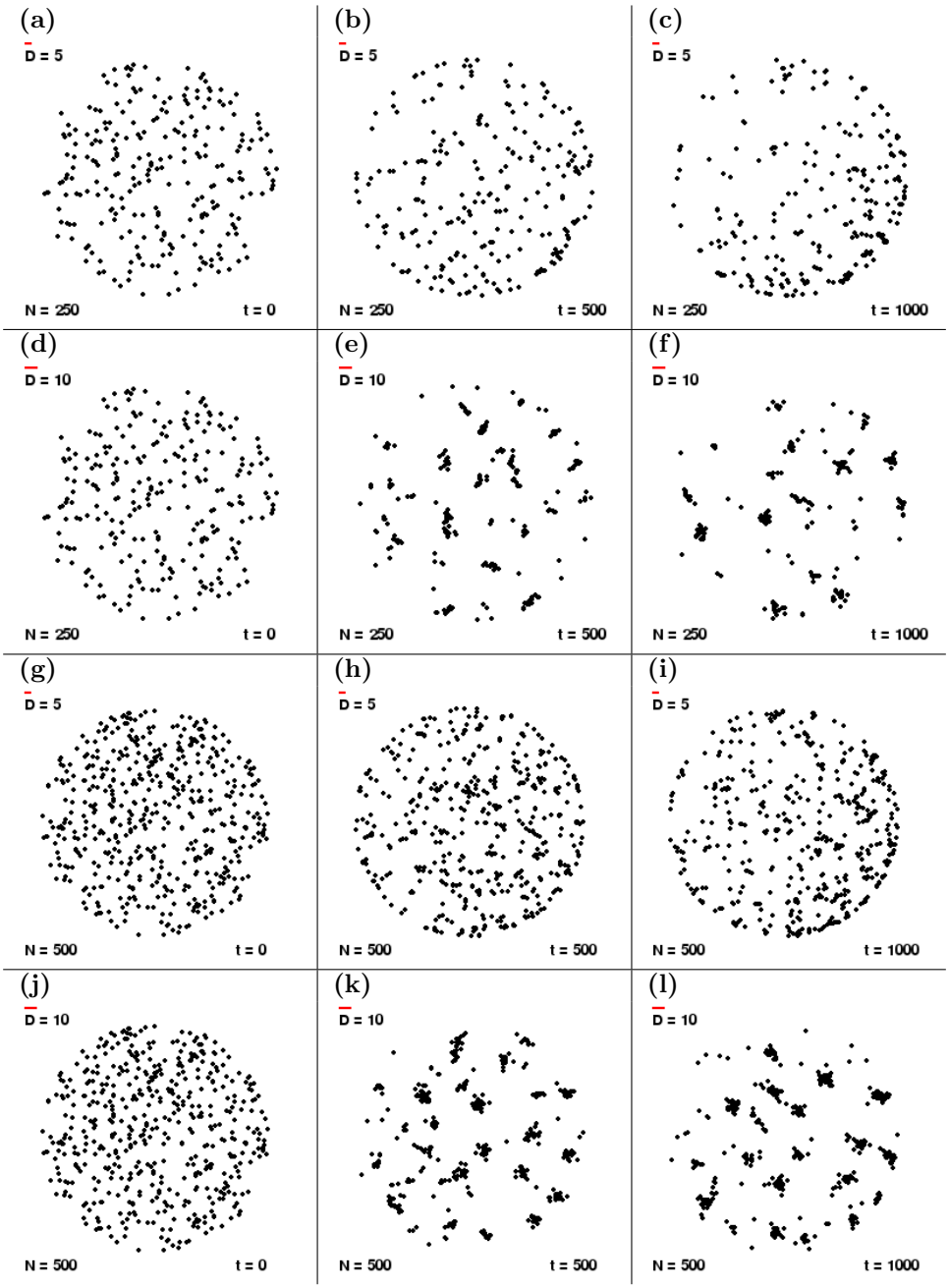

Figure 5: Global forcing model **A** at $t = 0, 500, 1000$ time steps with (a)-(c) $D = 5$, $N = 250$, (d)-(f) $D = 10$, $N = 250$, (g)-(i) $D = 5$, $N = 500$, and (j)-(l) $D = 10$, $N = 500$.

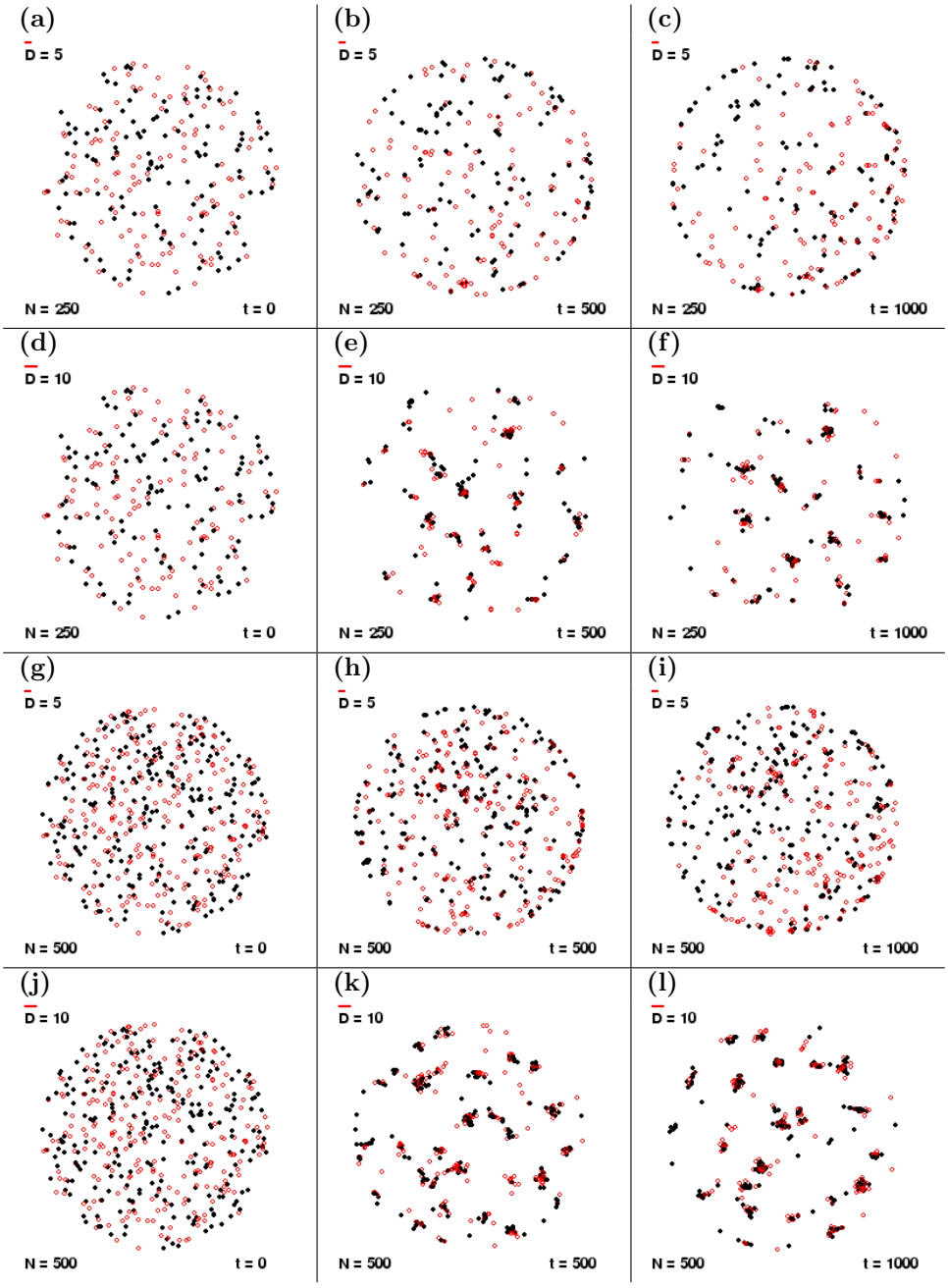

Figure 6: Global forcing model **B** with *leader* (red ○) to *normal* (black ●) cell ratio 1:1 at $t = 0, 500, 1000$ time steps with conditions (a)-(c) $D = 5$, $N = 250$, (d)-(f) $D = 10$, $N = 250$, (g)-(i) $D = 5$, $N = 500$, and (j)-(l) $D = 10$, $N = 500$.

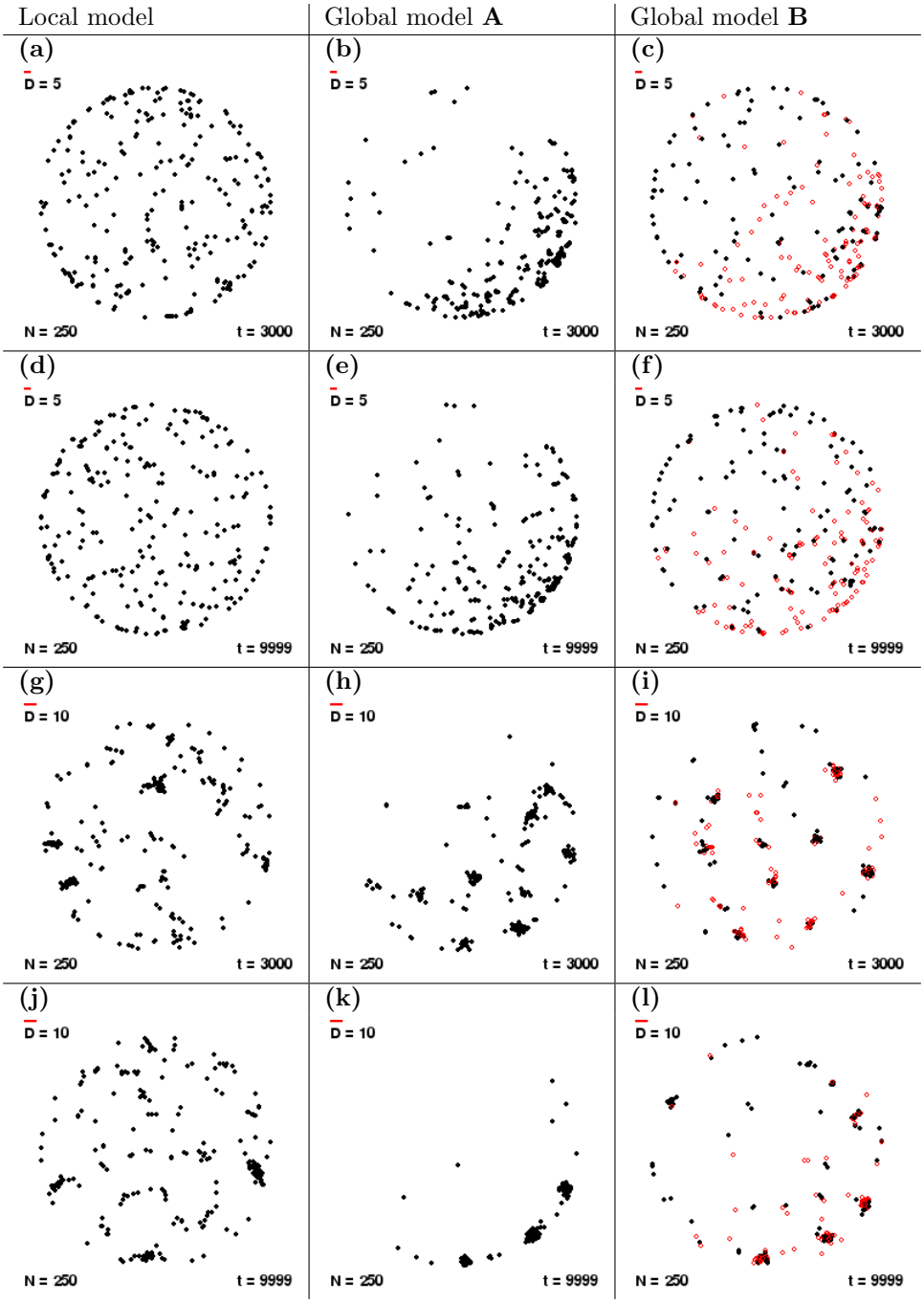

Figure 7: Long time simulations ($t = 3000$ and 9999) of each model for $N = 250$ particles with (a)-(f) $D = 5$ and (g)-(l) $D = 10$.

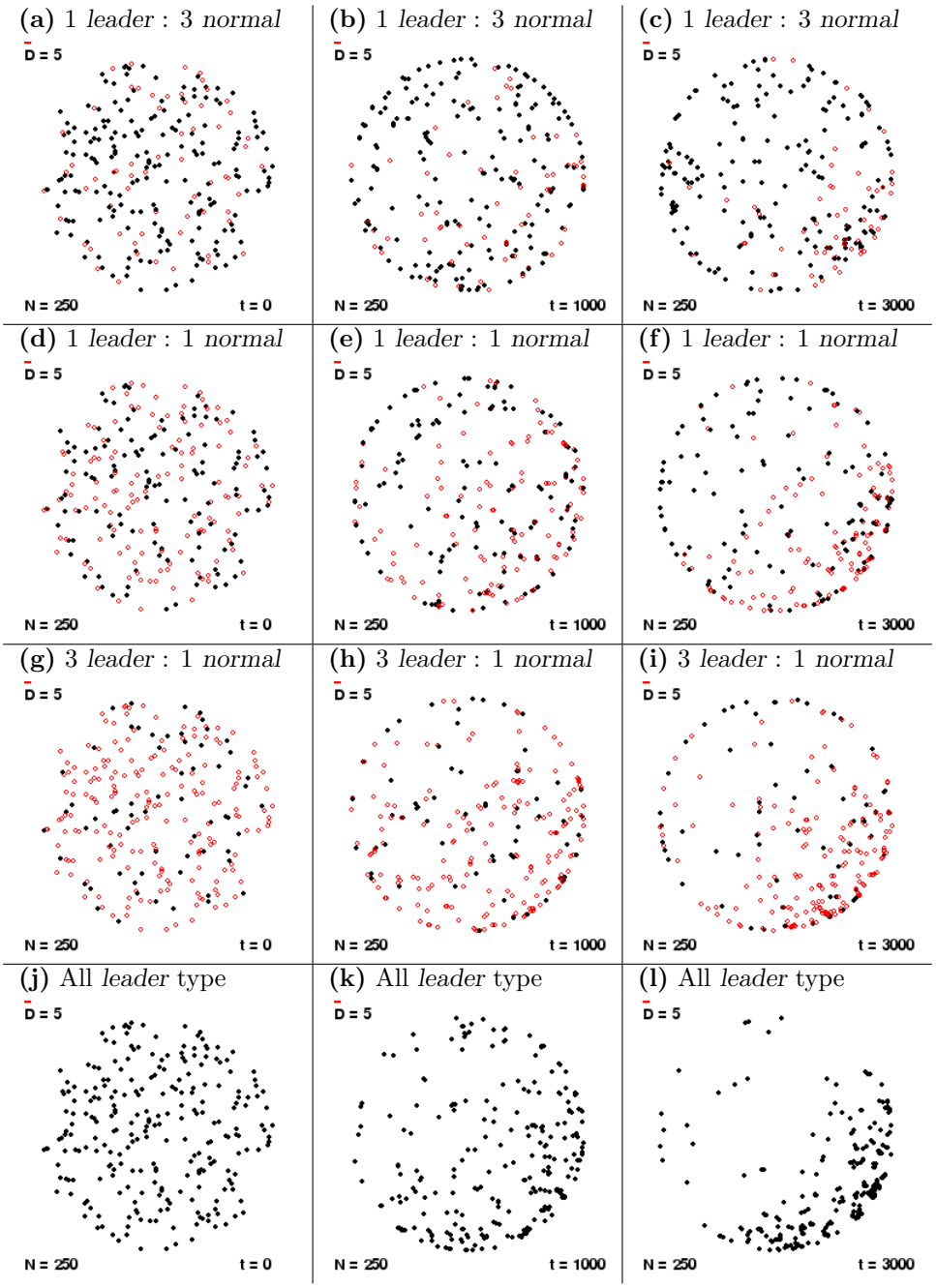

Figure 8: Simulations of global model **B** at $t = 0, 1000$, and 3000 time steps for $D = 5$ with various ratios of *leader* (red ○) to *normal* (black ●) cells: (a)-(c) 1 *leader* : 3 *normal*, (d)-(f) 1 *leader* : 1 *normal*, (g)-(i) 3 *leader* : 1 *normal* and (j)-(l) All *leader* cells, i.e. global model **A**